Proceedings of *RAGtime 17–19, 17–19/23–26 Oct., 1–5 Nov., 2015/2016/2017, Opava, Czech Republic*
Z. Stuchlík, G. Török and V. Karas, editors, Silesian University in Opava, 2017, pp. 33–46

Wave excitation at Lindblad resonances using the method of multiple scales

Jiří Horák

Astronomical Institute, Academy of Sciences, Boční II 141 31 Prague, Czech Republic

ABSTRACT
In this note, the method of multiple scales is adopted to the problem of excitation of non–axisymmetric acoustic waves in vertically integrated disk by tidal gravitational fields. We derive a formula describing a waveform of exited wave that is uniformly valid in a whole disk as long as only a single Lindblad resonance is present. Our formalism is subsequently applied to two classical problems: trapped p–mode oscillations in relativistic accretion disks and the excitation of waves in infinite disks.

Keywords: perturbation methods – disk dynamics

1 INTRODUCTION

A linear wave dynamics and wave excitation in fluid disks due to time–varying non–axisymmetric tidal fields have been extensively studied since publishing the seminal work on this subject by Goldreich and Tremaine (1979). In addition to small–amplitude long–scale non–resonant deformations of the disk, tides (originating in e.g. due to a companion star) may excite short–wavelength non–axisymmetric density waves at Lindblad resonances, where the frequency of a disturbing potential measured in a fluid frame matches the local epicyclic frequency.

Dynamics of a thin disk under the influence of the disturbing tidal field is described by following dimensionless equations

$$\frac{\partial u}{\partial t} + \Omega\frac{\partial u}{\partial \phi} - 2\Omega v + \epsilon_{\mathrm{d}}^2\frac{\partial h}{\partial r} = -\epsilon_\varphi \varphi'(r)\exp\left[\mathrm{i}(m\phi - \omega t)\right], \tag{1}$$

$$\frac{\partial v}{\partial t} + \Omega\frac{\partial v}{\partial \phi} + \frac{\kappa^2}{2\Omega}u + \frac{\epsilon_{\mathrm{d}}^2}{r}\frac{\partial h}{\partial \phi} = -\frac{\mathrm{i}m}{r}\epsilon_\varphi \varphi(r)\exp\left[\mathrm{i}(m\phi - \omega t)\right], \tag{2}$$

$$\frac{\partial h}{\partial t} + \Omega\frac{\partial h}{\partial \phi} + c_{\mathrm{s}}^2\left[\frac{1}{r\Sigma}\frac{\partial(r\Sigma u)}{\partial r} + \frac{1}{r}\frac{\partial v}{\partial \phi}\right] = 0. \tag{3}$$

Here, u and v are perturbations of the radial and tangential velocity, h is a perturbation of the enthalpy related to the wave, $\varphi(r)$ is a component of a disturbing gravitational potential, with azimuthal wavenumber m and the angular frequency ω, Ω and κ is the equilibrium orbital velocity and epicyclic frequency $\Omega = \kappa \propto r^{-3/2}$ for a Keplerian disk) and c_{s} is

978-80-7510-257-7

the constant sound speed (assuming the isothermal equation of state). All quantities are dimensionless, expressing ratios of corresponding dimensional physical quantities to their typical (characteristic) values. Radial distances are scaled by r_*, a characteristic radius that plays a role of a natural length unit. The angular frequency at this radius defines a scaling of all frequencies and introduces a natural time unit $t_* = 1/\Omega_*$. The velocity perturbations u and v are expressed in units $r_*\Omega_*$. On the other hand, the enthalpy perturbations h are of the order of a local sound speed and it is natural to express them in units of $c_{s*} = c_s(r_*)$. Finally, Σ expresses the density in units of $\Sigma_* = \Sigma(r_*)$ and a disturbing gravitational potential φ is rescaled by its typical value, say φ_*. Because we introduced c_{s*} and φ_* independently to r_* and Ω_*, two dimensionless parameters pops up in equations (1)–(3),

$$\epsilon_d \equiv \frac{c_{s*}}{r_*\Omega_*}, \quad \epsilon_\varphi \equiv \frac{\varphi_*}{r_*^2\Omega_*^2}. \tag{4}$$

The first one is proportional to the disk aspect ratio, $\epsilon_d \ll 1$ for thin disks. The second one expresses a relative importance of gravities of the central and perturbing object. The perturbation approach introduced in this note is appropriate in situations when both ϵ_d and ϵ_φ are much smaller then unity.

As shown by Goldreich and Tremaine (1979), a wave of the form of $\propto \exp[i(m\phi - \omega t)]$ is excited at radii, where

$$D \equiv \kappa^2 - (\omega - m\Omega)^2 = -[\omega - (m\Omega - \kappa)][\omega - (m\Omega + \kappa)] = 0, \tag{5}$$

from which we find $\omega = m\Omega \pm \kappa$. The upper/lower sign corresponds to the outer/inner Lindblad resonance. We assume that a single Lindblad resonance exists inside the disk and denote the corresponding radius $r = r_L$. Our task is to find a waveform corresponding to the excited wave.

2 SCALING THE VARIABLES, FAST RADIUS

We approach this problem using the method of multiple scales. In addition to the slow radial variable r, we introduce a fast radial coordinate x as

$$x \equiv \chi(r)/\delta, \tag{6}$$

where $\delta \ll 1$ is a free small parameter and $\chi(r)$ is a "normally" varying function of r (i.e. $\chi'(r) = O(1)$). Both δ and $\chi(r)$ will be determined later. We allow the solutions u, v and h to depend on both r and x. We just assume that derivatives of the solutions with respect to r and x does not change the order in δ, that is we assume that $\partial/\partial x$ and $\partial/\partial r$ applied to the solutions remains of the order of unity. Hence, variations with respect to x correspond to fast (oscillatory) changes, while those with respect r describe slow (secular) changes of the solutions (for example in the local wavelength).

The radial derivative $\partial/\partial r$ is substituted by

$$\frac{\partial}{\partial r} \to \frac{\partial}{\partial r} + \frac{\chi'}{\delta}\frac{\partial}{\partial x}. \tag{7}$$

In addition, we assume the dependence $\propto \exp[\mathrm{i}(m\phi - \omega t)]$ of the solution variables u, v and h on time and azimuth and rescale them as

$$u(r,\phi,t) = \epsilon_u \hat{u}(r,x) \mathrm{e}^{\mathrm{i}(m\phi-\omega t)}, \tag{8}$$

$$v(r,\phi,t) = \epsilon_u \hat{v}(r,x) \mathrm{e}^{\mathrm{i}(m\phi-\omega t)}, \tag{9}$$

$$h(r,\phi,t) = \epsilon_h \hat{h}(r,x) \mathrm{e}^{\mathrm{i}(m\phi-\omega t)}. \tag{10}$$

A relation of the additional scaling parameters δ, ϵ_u and ϵ_h to ϵ_φ and ϵ_d will be found using a dominant–balance argument. Introducing the Doppler–shifted frequency $\tilde{\omega}(r) = \omega - m\Omega(r)$, substituting (8)–(10) into (1)–(3) and factorizing out the time and azimuthal dependence, we obtain

$$\epsilon_u \left(-\mathrm{i}\tilde{\omega}\hat{u} - 2\Omega\hat{v}\right) + \frac{\epsilon_u \epsilon_h}{\delta}\chi' \frac{\partial \hat{h}}{\partial x} + \epsilon_\mathrm{d}^2 \epsilon_h \frac{\partial \hat{h}}{\partial r} = -\epsilon_\varphi \varphi', \tag{11}$$

$$\epsilon_u \left(\frac{\kappa^2}{2\Omega}\hat{u} - \mathrm{i}\tilde{\omega}\hat{v}\right) + \epsilon_\mathrm{d}^2 \epsilon_h \frac{\mathrm{i}m}{r}\hat{h} = -\epsilon_\varphi \frac{\mathrm{i}m}{r}\varphi, \tag{12}$$

$$-\,\mathrm{i}\epsilon_h \tilde{\omega}\hat{h} + \frac{\epsilon_u}{\delta} c_\mathrm{s}^2 \chi' \frac{\partial \hat{u}}{\partial x} + \epsilon_u c_\mathrm{s}^2 \left[\frac{1}{r\Sigma}\frac{\partial (r\Sigma\hat{u})}{\partial r} + \frac{\mathrm{i}m}{r}\hat{v}\right] = 0. \tag{13}$$

The first two equations are algebraic in $\hat{u}$ and $\hat{v}$. Eliminating $\hat{u}$ from them, we find

$$\mathrm{i}\epsilon_u D\hat{u} + \frac{\epsilon_\mathrm{d}^2 \epsilon_h}{\delta}\tilde{\omega}\chi' \frac{\partial \hat{h}}{\partial x} + \epsilon_\mathrm{d}^2 \epsilon_h \left(\tilde{\omega}\frac{\partial \hat{h}}{\partial r} - \frac{2m\Omega}{r}\hat{h}\right) = -\epsilon_\varphi \left(\tilde{\omega}\varphi' - \frac{2m\Omega}{r}\varphi\right). \tag{14}$$

The variable $D \equiv \kappa^2 - \tilde{\omega}^2$ vanishes at $r = r_\mathrm{L}$, a position of Lindblad resonance. We want our solution to be valid also at this radius. Therefore it is reasonable to set

$$D = \chi(r)\mathcal{D}(r) = \delta \mathcal{D}(r) x \tag{15}$$

with

$$\chi(r_\mathrm{L}) = 0. \tag{16}$$

Here $\mathcal{D}(r)$ is a positive function of the slow radius r of the order of unity. Therefore, in the vicinity of r_L, $\chi(r)$ is either increasing or decreasing function depending on the type of the Lindblad resonance. The inner Lindblad resonance corresponds to $\chi'(r_\mathrm{L}) > 0$, while $\chi'(r_\mathrm{L}) < 0$ for the the outer one. In the latter case, x increases with decreasing r as can be seen from equation (6). Hence, we adopt a convention of x being negative in the wave propagation region and positive in the wave evanescent region.

We next proceed with the dominant balance argument. We identify the essential terms in the governing equations and adjust the small parameters ϵ_u, ϵ_h and δ accordingly, so that they appear in the leading order of the expansion. In the case of equation (13), it is clear that the first term must balance the second one, because the third one is always less important than the second. Keeping just one of the first two terms in the leading order would result in trivial solution (either $\hat{h}$ or $\partial\hat{u}/\partial x$ would be zero in the leading order).

Hence, we require $\epsilon_u = \mathcal{O}(\epsilon_h/\delta)$. The same argument applies to the equation (14), where we again has to balance the first and the second term in the leading approximation in order to keep a nontrivial dependence of the leading–order solution on the fast variable x. This leads to a requirement $\epsilon_u = \mathcal{O}(\epsilon_{\mathrm{d}}^2\epsilon_h/\delta^2)$. Finally, we want the forcing terms in equation (14) that involves the gravitational–field perturbation to which the disk reacts to appear in the leading order as well, this imply $\epsilon_{\mathrm{u}} = \mathcal{O}(\epsilon_\varphi/\delta)$. To sum up, we introduce the scaling

$$\delta = \epsilon_{\mathrm{d}}^{2/3}, \quad \epsilon_u = \frac{\epsilon_\varphi}{\delta}, \quad \epsilon_h = \frac{\epsilon_\varphi}{\delta^2}. \tag{17}$$

The magnitude of all terms in equations (14), (12) and (13) is then proportional to ϵ_φ, that can be factorized out. Upon dividing equation (14) by $\mathcal{D}(r)$, we obtain

$$\mathrm{i}x\hat{u} + \frac{\tilde{\omega}\chi'}{\mathcal{D}}\frac{\partial\hat{h}}{\partial x} + \frac{\delta}{\mathcal{D}}\left(\tilde{\omega}\frac{\partial\hat{h}}{\partial r} - \frac{2m\Omega}{r}\hat{h}\right) = \Phi(r) \tag{18}$$

$$\frac{\kappa^2}{2\Omega}\hat{u} - \mathrm{i}\tilde{\omega}\hat{v} + \delta\frac{\mathrm{i}m}{r}\hat{h} = -\delta\frac{\mathrm{i}m}{r}\varphi, \tag{19}$$

$$-\mathrm{i}\tilde{\omega}\hat{h} + c_{\mathrm{s}}^2\chi'\frac{\partial\hat{u}}{\partial x} + \delta c_{\mathrm{s}}^2\left[\frac{1}{r\Sigma}\frac{\partial(r\Sigma\hat{u})}{\partial r} + \frac{\mathrm{i}m}{r}\hat{v}\right] = 0, \tag{20}$$

where

$$\Phi(r) \equiv \frac{1}{\mathcal{D}}\left(\tilde{\omega}\varphi' - \frac{2m\Omega}{r}\varphi\right). \tag{21}$$

Finally, for the reasons that will be obvious later, it is necessary to involve the fast scale x also in the slowly varying function $\Phi(r)$ on the right–hand side of equation (18). Whe therefore rewrite it as

$$\Phi(r) = \Phi_0(r) + \chi(r)\Phi_1(r) \equiv \Phi_0(r) + \delta\Phi_1(r)x. \tag{22}$$

The exact form of function $\Phi_0(r)$ will be determined later, once determined the function $\Phi_1(r)$ is given by

$$\Phi_1(r) = \frac{1}{\chi(r)}\left[\Phi(r) - \Phi_0(r)\right]. \tag{23}$$

Equations (18)–(20) are now suitable for the perturbative solution.

3 PERTURBATIVE SOLUTION

We assume the solutions $\hat{u}$, $\hat{v}$ and $\hat{h}$ of the form of power series in terms of δ,

$$\hat{u} = u_0 + \delta u_1 + \ldots, \quad \hat{v} = v_0 + \delta v_1 + \ldots, \quad \hat{h} = h_0 + \delta h_1 + \ldots. \tag{24}$$

Substituting these expansions into equations (18)–(20) and comparing the terms of the same order of δ, we obtain equations leading the approximations of various orders. For our purposes it is sufficient to consider only zeroth order (leading) and first order equations.

3.1 Zeroth order

The zeroth–order equations are

$$\mathrm{i}xu_0 + \frac{\tilde{\omega}\chi'}{\mathcal{D}}\frac{\partial h_0}{\partial x} = \Phi_0, \quad \frac{\kappa^2}{2\Omega}u_0 - \mathrm{i}\tilde{\omega}v_0 = 0, \quad -\mathrm{i}\tilde{\omega}h_0 + c_\mathrm{s}^2\chi'\frac{\partial u_0}{\partial x} = 0. \tag{25}$$

Hence,

$$\frac{(c_\mathrm{s}\chi')^2}{\mathcal{D}}\frac{\partial^2 u_0}{\partial x^2} - xu_0 = \mathrm{i}\Phi_0. \tag{26}$$

We still have a freedom to chose $\chi(r)$. A natural choice is to put

$$\frac{(c_\mathrm{s}\chi')^2}{\mathcal{D}} = \frac{\chi\,(c_\mathrm{s}\chi')^2}{D} = 1, \tag{27}$$

what together with the condition (16) leads to

$$\chi(r) = \left[\frac{3}{2}\int_{r_0}^{r} q(r')\mathrm{d}r'\right]^{2/3}, \quad q(r) = \frac{\sqrt{D}}{c_\mathrm{s}}. \tag{28}$$

This brings the equation (26) to the form

$$\frac{\partial^2 u_0}{\partial x^2} - xu_0 = \mathrm{i}\Phi_0, \tag{29}$$

which is just the inhomogeneous Airy equation. Its general solution reads

$$u_0(r,x) = A(r)\mathrm{Ai}(x) + B(r)\mathrm{Bi}(x) - \mathrm{i}\pi\Phi_0(r)\mathrm{Gi}(x), \tag{30}$$

where $\mathrm{Ai}(x)$, $\mathrm{Bi}(x)$ and $\mathrm{Gi}(x)$ are Airy functions and $A(r)$ and $B(r)$ are integration constants whose dependence on the slow variable will be determined in the next order of approximation. The other variables follow easily,

$$v_0 = \frac{\mathrm{i}\kappa^2}{2\Omega\tilde{\omega}}u_0, \quad h_0 = -\frac{\mathrm{i}c_\mathrm{s}^2\chi'}{\tilde{\omega}}\frac{\partial u_0}{\partial x}. \tag{31}$$

3.2 First order

In the first order, we have to solve following equations

$$\mathrm{i}xu_1 + \frac{\tilde{\omega}\chi'}{\mathcal{D}}\frac{\partial h_1}{\partial x} = \frac{\tilde{\omega}}{\mathcal{D}}\frac{\partial h_0}{\partial r} + \frac{2m\Omega}{r}h_0 + x\Phi_1(r), \tag{32}$$

$$\frac{\kappa^2}{2\Omega}u_1 - \mathrm{i}\tilde{\omega}v_1 = -\frac{\mathrm{i}m}{r}\varphi, \tag{33}$$

$$-\mathrm{i}\tilde{\omega}h_1 + c_\mathrm{s}^2\chi'\frac{\partial u_1}{\partial x} = -c_\mathrm{s}^2\left[\frac{1}{r\Sigma}\frac{\partial(r\Sigma u_0)}{\partial r} + \frac{\mathrm{i}m}{r}v_0\right]. \tag{34}$$

After some algebra and using the equation (28), one finds

$$\frac{\partial^2 u_1}{\partial x^2} - x u_1 = -\frac{1}{\chi'}\left(\frac{\mathrm{d}}{\mathrm{d}r}\ln\frac{r\Sigma\chi'}{\tilde{\omega}^2}\right)\frac{\partial u_0}{\partial x} - \frac{2}{\chi'}\frac{\partial^2 u_0}{\partial r\partial x} + \mathrm{i}x\Phi_1(r). \tag{35}$$

When the zeroth–order solutions are substituted into this equation, one finally obtains

$$\begin{aligned}\frac{\partial^2 u_1}{\partial x^2} - x u_1 = &-\frac{2}{\chi'\psi}\left[\frac{\mathrm{d}(\psi A)}{\mathrm{d}r}\mathrm{Ai}'(x) + \frac{\mathrm{d}(\psi B)}{\mathrm{d}r}\mathrm{Bi}'(x) - \mathrm{i}\pi\frac{\mathrm{d}(\psi\Phi_0)}{\mathrm{d}r}\mathrm{Gi}'(x)\right]\\ &+ \mathrm{i}x\Phi_1(r)\end{aligned} \tag{36}$$

with

$$\psi(r) \equiv \frac{\sqrt{r\Sigma\chi'}}{\tilde{\omega}} = \frac{\sqrt{r\Sigma q}}{\tilde{\omega}}\chi^{-1/4}. \tag{37}$$

We are interested in a particular solution of this equation as the solutions of the homogeneous equation can be absorbed into zeroth order approximation u_0. Due to linearity, a particular solution will be sum of particular solutions to all individual terms on the right–hand side. The first three terms consist of slowly varying functions of r multiplied by derivatives of Airy functions. The corresponding particular solutions will be thus given by the Airy functions multiplied by $x/2$. This will cause non–uniformity in our expansion at $x = \mathcal{O}(1/\delta)$, when the first order approximation u_1 becomes equally important as the zeroth order one u_0. Our strategy is therefore to introduce suitably varying functions $A(r)$, $B(r)$ and $\Phi_0(r)$ in order to kill these terms and avoid the non–uniformity of the final expansion. This leads us to require $A(r)$, $B(r)$ and $\Phi_0(r)$ to vary as $\propto \psi(r)^{-1}$,

$$A(r) = \frac{a}{\psi(r)}, \quad B(r) = \frac{b}{\psi(r)}, \quad \Phi_0(r) = \frac{\psi_{\mathrm{L}}\Phi_{\mathrm{L}}}{\psi(r)}, \tag{38}$$

where a and b are constants that must be determined from boundary conditions and the index 'L' denotes evaluation of the corresponding quantity at r_{L}. Note that

$$\psi_{\mathrm{L}}\Phi_{\mathrm{L}} = \left(\frac{\sqrt{r\Sigma}}{\kappa}\right)_{\mathrm{L}}\left(\tilde{\omega}\varphi' - \frac{2m\Omega}{r}\varphi\right)_{\mathrm{L}}. \tag{39}$$

Equation (38) describes slow (secular) evolution of the amplitudes of individual Airy functions with changing radius. At this point, it is also obvious why we imposed the decomposition (22) on the potential function $\Phi(r)$. Keeping it in its original form in the zeroth–order equations would lead to appearance of the unavoidable secular term $\propto x\Phi(r)\mathrm{Gi}(x)$ in the first–order approximation and would result in the non–uniform expansion.

The particular solution of equation (36) after elimination of the secular terms using (38) reads

$$u_1(r,x) = -\mathrm{i}\Phi_1(r) = -\frac{\mathrm{i}}{\chi(r)}\left[\Phi(r) - \frac{\psi_{\mathrm{L}}\Phi_{\mathrm{L}}}{\psi(r)}\right]. \tag{40}$$

3.3 Uniform approximation

Putting equations (30), (38), (28) and (40) together, we find the final solution valid up to the first order in the perturbation parameter δ,

$$\hat{u}(r,x) = \frac{\tilde{\omega}}{\sqrt{r\Sigma q}}\chi^{1/4}\left[a\mathrm{Ai}(x) + b\mathrm{Bi}(x) - \mathrm{i}\pi\psi_{\mathrm{L}}\Phi_{\mathrm{L}}\mathrm{Gi}(x)\right] - \frac{\mathrm{i}\delta}{\chi(r)}\left[\Phi(r) - \frac{\psi_{\mathrm{L}}\Phi_{\mathrm{L}}}{\psi(r)}\right]. \tag{41}$$

The expression (41) represents an uniform approximation of the waveform of perturbation that is valid in the whole disk as far as a single Lindblad resonance is present. The case of several Lindblad resonances will be treated in the section 4.3. The constants a and b can be chosen freely according to the boundary conditions imposed on the perturbation at disk boundaries. In the following sections 4.1 and 4.2 we give two specific examples.

4 APPLICATIONS

4.1 Frequencies of trapped p–modes in relativistic disks

In thin relativistic disks, the acoustic waves can be trapped between the inner edge of the disk and the inner Lindblad resonance establishing the standing wave patterns, so called p–modes. The frequencies of these modes take discrete values ω_n that are given by physical conditions of the flow at the disk inner edge located at the marginally stable orbit r_{ms} (Kato and Fukue, 1980; Nowak and Wagoner, 1991; Wagoner, 1999). Thus measuring their values may serve as another important probe into physical properties of the accreted matter in the very vicinity of relativistic objects. The frequencies of the lowest order p–modes (i.e. those with low number of nodes in the radial direction) are always close to $m\Omega(r_{\mathrm{ms}})$ and their propagation regions are rather narrow. On the other hand they occupy portions of a disk from which most of the radiation emerges and thus they may still be observed. Moreover, if the underlying compact object is a neutron star, these modes may likely strongly modulate accretion rate of a falling matter and therefore contribute significantly to the variability of the emission from its surface (Paczynski, 1987; Horák, 2005; Abramowicz et al., 2007).

Here we derive an approximate formula for the discrete frequency spectra of both, axisymmetric and nonaxisymmetric p–modes. For simplicity, we assume that the disk is terminated at r_{ms} and fix the inner boundary condition to be $u(r_{\mathrm{ms}}) = 0$. As we consider free oscillations, we put $\Phi(r) = 0$ and $\Phi_{\mathrm{L}} = 0$ in equation (41). Because the solution has to be bounded, we also cut off its divergent part proportional to $\mathrm{Bi}(x)$ by putting $b = 0$. The waveform (eigenfunction) of the p–mode is thus roughly described by

$$\hat{u}(r,x) = \frac{a\tilde{\omega}}{\sqrt{r\Sigma q}}\chi^{1/4}\mathrm{Ai}(x), \tag{42}$$

where a is now an arbitrary normalization constant and x is given by equations (6) and (28).

The inner Lindblad resonance corresponds to $x = 0$, while $x = x_{\mathrm{ms}}$ corresponds to the disk inner boundary. The value of x_{ms} depends on the frequency ω of the oscillations, hence

$x_{\rm ms} = x_{\rm ms}(\omega)$. Because we demand vanishing velocity perturbation at the inner edge, the discrete modes have to correspond to the points x_n, where the Airy function vanishes. Thus

$$x_{\rm ms}(\omega_n) = x_n, \quad \mathrm{Ai}(x_n) = 0. \tag{43}$$

From the theory of Airy functions, it follows that

$$x_n \approx -\left[\frac{3\pi}{8}(4n+3)\right]^{2/3}, \quad n = 0, 1, 2, \dots. \tag{44}$$

Therefore, our task is to evaluate the function $x_{\rm ms}(\omega)$. As we expect ω close to $m\Omega_{\rm ms}$, we put

$$\omega = m\Omega_{\rm ms} + \delta^{\alpha}\omega_1, \tag{45}$$

where $\alpha > 0$ will be specified later on. Close to $r_{\rm ms}$ the orbital and epicyclic frequencies can be approximated as

$$\Omega(r) \approx \Omega_{\rm ms} + \Omega_1 (r - r_{\rm ms}), \quad \kappa^2(r) \approx \kappa_1^2 (r - r_{\rm ms}), \tag{46}$$

where

$$\Omega_1 \equiv \left(\frac{\mathrm{d}\Omega}{\mathrm{d}r}\right)_{\rm ms}, \quad \kappa_1^2 \equiv \left(\frac{\mathrm{d}\kappa^2}{\mathrm{d}r}\right)_{\rm ms}. \tag{47}$$

Introducing a scaled variable ρ using $r = r_{\rm ms} + \delta^{\beta}\rho$, we obtain

$$D = \kappa^2 - \tilde{\omega}^2 = \delta^{\beta}\kappa_1^2\rho - \delta^{2\alpha}\omega_1^2 - 2\delta^{\alpha+\beta}m\Omega_1\omega_1\rho - \delta^{2\beta}m\Omega_1^2\rho^2. \tag{48}$$

The last two terms are obviously sub–dominant with respect to the first one and will be neglected further on. At the Lindblad resonance $D = 0$. This can be achieved only by balancing the first two terms giving $\beta = 2\alpha$. In terms of ρ the position of the resonance corresponds to

$$\rho_{\rm L} = \frac{\omega_1^2}{\kappa_1^2}. \tag{49}$$

The integral in equation (28) may be therefore evaluated as

$$\int_{r_0}^{r_{\rm ms}} \frac{\sqrt{D}}{c_{\rm s}}\mathrm{d}r' = -\frac{\delta^{3\beta/2}}{c_{\rm s}}\int_0^{\rho_{\rm L}} \sqrt{\kappa_1^2\rho' - \omega_1^2}\,\mathrm{d}\rho' = -\delta^{3\beta/2}\frac{2\mathrm{i}\omega_1^3}{3c_{\rm s}\kappa_1^2}. \tag{50}$$

Therefore,

$$x_{\rm ms}(\omega) = -\frac{\omega_1^2}{\left(c_{\rm s}\kappa_1^2\right)^{2/3}}, \tag{51}$$

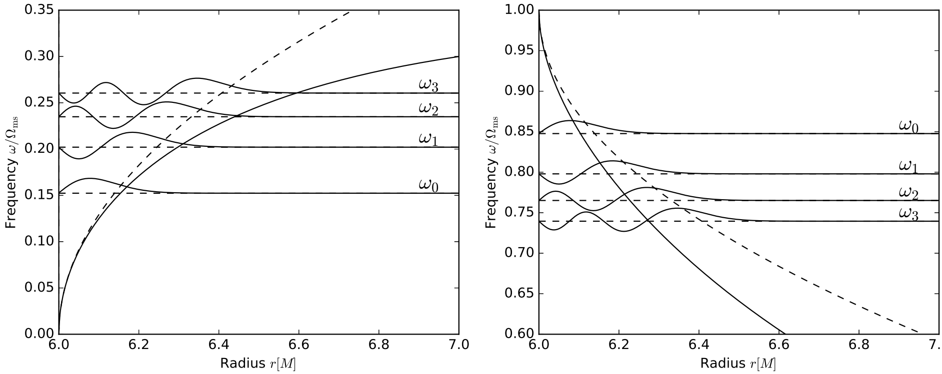

Figure 1. The spectrum of the lowest–order trapped axisymmetric p–modes in a relativistic thin disk surrounding the Schwarzschild black hole according to formula (52). The left and right panel shows the case of the axisymmetric and non–axisymmetric ($m = 1$) modes, respectively. The oscillations are trapped between the disk inner edge at $r = r_{\rm ms} = 6M$ and the inner Lindblad resonance located at positions, where the Doppler–shifted oscillation frequency $|\tilde{\omega}|$ matches the local epicyclic frequency $\kappa(r)$ (shown by solid lines). The approximate positions of the inner Lindblad resonance used in the calculations are shown by the dashed lines. The frequencies of the four discrete modes are calculated for the sound speed $c_{\rm s} = 10^{-3}(r\Omega)_{\rm ms}$.

where we have set $\beta = 1$, in order to obtain $x_{\rm ms}$ of the order of unity. Finally, from the conditions (43) and (44) and using (45) we get,

$$\omega = m\Omega_{\rm ms} \pm \epsilon_{\rm d}^{1/3} \left[\frac{3\pi}{8} (4n+3) \left(c_{\rm s} \kappa_1^2 \right) \right]^{1/3} . \tag{52}$$

The eigenfrequencies and eigenfunctions calculated using (52) and (42) for the lowest–order axisymmetric modes ($n \le 4$) are shown in Fig. 1. For the epicylic frequency, we have used $\kappa(r) = (1 - r_{\rm ms}/r)^{1/2}\Omega(r)$ with $r_{\rm ms} = 6M$ suitable for the Schwarzschild black hole. The dashed line shows positions of the inner Lindblad resonance based on our approximation of $\kappa(r)$ using the square–root function (see eq. (46)). The formula describes the eigenfrequencies well the lowest–order modes with small propagation regions, as the trapping cavity opens up, our simple approximation of the epicyclic frequency ceases to describe its real profile and the formula (52) fails. However, a higher precision could be achieved by considering additional terms in the expansions of $\kappa(r)$ and $\Omega(r)$.

4.2 Excitation of waves in infinite disks

Another application concerns excitation of waves in the infinite disk by a time and azimuthally dependent tidal field (for example due to orbital motion of a secondary star). The solution is described by equation (41) with $\varphi(r)$ corresponding to a Fourier component of the tidal potential that changes as $\exp(m\phi - \omega t)$. In the case of a secondary orbiting on the strictly circular orbit $\omega = m\Omega_*$ with Ω_* being the orbital period. The constants a and b in the equation (41) has to be fixed by boundary condition. For this, it is useful to explore asymptotic behavior of the solution far from the resonance. Suppose for the moment that wave is excited at the inner Lindblad resonance. The waves may propagate only at smaller radii where D is negative. Far from the resonance, at $r \ll r_{\mathrm{L}}$, the solution behaves as

$$
\begin{aligned}
\hat{u}(r,x) \sim \delta^{1/4}\frac{\tilde{\omega}}{\sqrt{4\pi r\Sigma k}} &\left\{[a-\pi\psi_{\mathrm{L}}\Phi_{\mathrm{L}}-\mathrm{i}b]\exp\left[-\frac{\mathrm{i}}{\epsilon_{\mathrm{d}}}\left(\int_r^{r_{\mathrm{L}}} k\,\mathrm{d}r' + \frac{\pi}{4}\right)\right]\right. \\
&\left. + [a+\pi\psi_{\mathrm{L}}\Phi_{\mathrm{L}}+\mathrm{i}b]\exp\left[\frac{\mathrm{i}}{\epsilon_{\mathrm{d}}}\left(\int_r^{r_{\mathrm{L}}} k\,\mathrm{d}r' - \frac{\pi}{4}\right)\right]\right\} \\
&+ \frac{\delta}{D}\left(\tilde{\omega}\varphi' - \frac{2m\Omega}{r}\varphi\right),
\end{aligned}
\tag{53}
$$

where $k = -\mathrm{i}q = \sqrt{-D}/c_{\mathrm{s}}$. The solution has three components. The first two terms in the brace bracket describe ingoing and outgoing waves with respect to the Lindblad resonance. The energy tcarried by the waves is transported with group velocity $c_{\mathrm{g}} = \mathrm{d}\omega/\mathrm{d}k = (k/\tilde{\omega})c_{\mathrm{s}}^2$. The sign of c_{g} determines whether the wave is ingoing or outgoing with respect to the resonance. In our case of the inner Lindblad resonance and $\omega > 0$, the first term corresponds to the ougoing wave and the second one to the ingoing wave (compare to Zhang and Lai, 2006). The last third term represents a non–resonant non–wave response of the disk ('deformation') due to the tidal field. On the other side of the resonance, we have for $r \gg r_{\mathrm{L}}$,

$$
\begin{aligned}
\hat{u}(r,x) \sim \delta^{1/4}\frac{\tilde{\omega}}{\sqrt{\pi r\Sigma q}} &\left[\frac{a}{2}\exp\left(-\frac{1}{\epsilon_{\mathrm{d}}}\int_{r_{\mathrm{L}}}^{r} q\,\mathrm{d}r'\right) + b\exp\left(\frac{1}{\epsilon_{\mathrm{d}}}\int_{r_{\mathrm{L}}}^{r} q\,\mathrm{d}r'\right)\right] \\
&+ \frac{\delta}{D}\left(\tilde{\omega}\varphi' - \frac{2m\Omega}{r}\varphi\right),
\end{aligned}
\tag{54}
$$

The solution comprises of two exponentials and the non–wave response that has the same form as in the other region.

A natural step is to put $b = 0$, what kills the divergent part of the solution (54) in the wave–evanescent region. Other constraint that fixes the constant a is imposed in wave–propagation region on (53). A traditional approach is to assume that the excited wave can propagate freely toward smaller radii, where it is either absorbed or damped by other physical processes like viscosity or turbulence. Then one requires the ingoing–wave part of the solution (53) to vanish what gives $a = \pi\psi_{\mathrm{L}}\Phi_{\mathrm{L}}$. The uniform approximation of the wave part of the solution then becomes

$$
\hat{u}_{\mathrm{wave}}(r,x) = \frac{\pi\tilde{\omega}}{\sqrt{r\Sigma q}}\psi_{\mathrm{L}}\Phi_{\mathrm{L}}\chi^{1/4}\left[\mathrm{Ai}(x) - \mathrm{i}\mathrm{Gi}(x)\right]. \tag{55}
$$

In a more general case when the waves can be partially reflected back towards the resonance, let us introduce the complex reflectivity as a ratio of the ingoing and outgoing (i.e. outgoing and ingoing with respect to a reflector) wave amplitudes,

$$
R \equiv \frac{a-\pi\psi_{\mathrm{L}}\Phi_{\mathrm{L}}}{a+\pi\psi_{\mathrm{L}}\Phi_{\mathrm{L}}}. \tag{56}
$$

Then

$$a = \frac{1+R}{1-R}\pi\psi_{\rm L}\Phi_{\rm L} \tag{57}$$

and

$$\hat{u}_{\rm wave}(r,x) = \frac{\pi\tilde{\omega}}{\sqrt{r\Sigma q}}\psi_{\rm L}\Phi_{\rm L}\chi^{1/4}\left[\frac{1+R}{1-R}{\rm Ai}(x) - {\rm i}{\rm Gi}(x)\right]. \tag{58}$$

We observe that in absence of the forcing ($\Phi_{\rm L} = 0$), the solution (58) is trivial, $\hat{u}_{\rm wave}(r,x) = 0$, unless $R = 1$. The case $R = 1$ corresponds to the situation when there exists a free oscillation mode whose eigenfrequency equals the frequency of the forcing and has to be treated in a different way.

4.3 Asymptotic matching

Finally, few words on the possibility of using our approach in the cases when there are more than one Lindblad resonance in the disk. This is typically the case of relativistic disks, where the axisymmetric p–mode oscillations with frequencies close to the maximum of the epicylic frequency can penetrate the potential barrier and carry some energy out from the trapping region. Clearly, the solution (41) cannot be applied to these situations, because the variable x does not know about the presence of the other resonances. Several attempts of the author to use non–monotonic functions instead of the always increasing or decreasing function $\chi(r)$ have not provided a reasonably simple way of calculations yet. Hence, so far the only way how to treat these situations is asymptotic matching of individual expressions (41) far from the resonances.

In order to demonstrate this procedure, let us consider a particular case of two Lindblad resonaces (inner and outer) located at radii r_1 and r_2 ($r_1 < r_2$). The wave–evanescent region corresponds to the interval (r_1, r_2), the regions corresponding to $r < r_1$ and $r > r_2$ allows waves to propagate freely. The solution (41) describing a single Lindblad resonance can be applied on both the inner and outer resonance. Denote $\hat{u}_1$ the solution corresponding to the inner resonance and $\hat{u}_2$ the solution corresponding to the outer one. The inner solution $\hat{u}_1$ is valid for $r < r_2$; close to r_2, $\hat{u}_1$ breaks down because of presence of the outer resonance. Similarly the solution $\hat{u}_2$ is valid for $r > r_1$. The evanescent region is the overlap, where both solutions are valid. Let us consider a radius r from the evanescent region, not too close to its boundaries. At this radius, the wave part of the solution $\hat{u}_1$ behaves as

$$\hat{u}_{1,\rm wave}(r,x) \sim \frac{\delta^{1/4}\tilde{\omega}}{\sqrt{\pi r\Sigma q}}\left[\frac{a_1}{2}\exp\left(-\frac{1}{\epsilon_{\rm d}}\int_{r_1}^{r} q\,{\rm d}r'\right) + b_1\exp\left(\frac{1}{\epsilon_{\rm d}}\int_{r_1}^{r} q\,{\rm d}r'\right)\right] \tag{59}$$

and similarly

$$\hat{u}_{2,\rm wave}(r,x) \sim \frac{\delta^{1/4}\tilde{\omega}}{\sqrt{\pi r\Sigma q}}\left[\frac{a_2}{2}\exp\left(-\frac{1}{\epsilon_{\rm d}}\int_{r}^{r_2} q\,{\rm d}r'\right) + b_2\exp\left(\frac{1}{\epsilon_{\rm d}}\int_{r}^{r_2} q\,{\rm d}r'\right)\right]. \tag{60}$$

By putting $\hat{u}_{1,\rm wave} = \hat{u}_{2,\rm wave}$, we obtain a relation between the constants a_1, b_1 and a_2, b_2,

$$a_2 = 2\Psi_{12}b_1, \quad b_2 = \frac{1}{2}\Psi_{12}^{-1}a_1, \quad \Psi_{12} \equiv \exp\left(\frac{1}{\epsilon_{\rm d}}\int_{r_1}^{r_2} q\,{\rm d}r'\right). \tag{61}$$

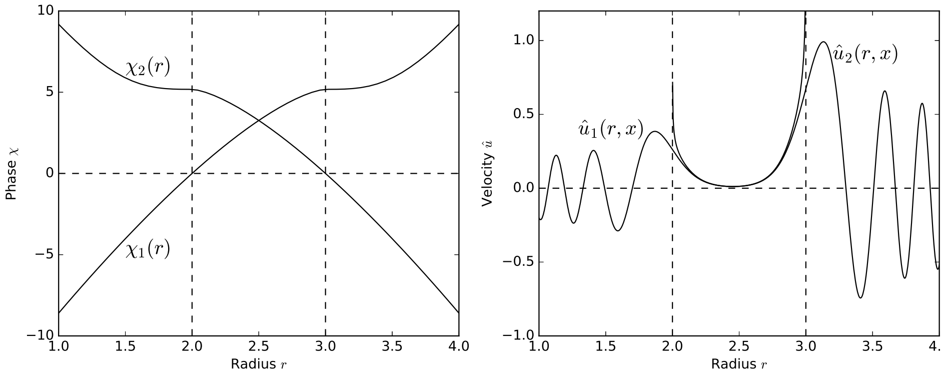

Figure 2. Example of matching the single–resonance solutions (41) in the case when two Lindblad resonances are present. The inner and outer Linblad resonance are located at $r_1 = 2$ and $r_2 = 3$, respectivelly (the radii are in arbitrary units r_*). For simplicity, we have assumed that $D = -(r - r_1)(r - r_2)$, $r\Sigma$ = const and c_s to be 5% of the orbital velocity at r_1. Left panel shows the individual phase functions $\chi_1(r)$ and $\chi_2(r)$ calculated according to equation (28). The right panel shows the solutions $\hat{u}_1(r,x)$ and $\hat{u}_2(r,x)$ for $a_1 = 2$, $b_1 = 0.001$ and a_2 and b_2 calculated using equation (61). Well inside the evanscent region between the resonances, these two solutions coincide and one may switch from the one to another.

The relation between the functions $\chi_1(r)$ and $\chi_2(r)$ is

$$\chi_2 = \left(\frac{3}{2}\ln\Psi_{12} - \chi_1^{3/2}\right)^{2/3}. \tag{62}$$

An example of the matching procedure is shown in Fig. 2. In practice, one builds up the solution $\hat{u}_1(r,x)$ and $\hat{u}_2(r,x)$ independently using (41) and (28). Then constants a and b are fixed so that they satisfy relations (61). And finally the solutions $\hat{u}_1(r,x)$ and $\hat{u}_2(r,x)$ are connected at an arbitrary radius r_m, well inside the evanescent region. The response of the disk is thus given by a piecewise function,

$$\hat{u}(r,x;a,b) = \begin{cases} \hat{u}_1(r,x;a,b), & r < r_\mathrm{m}, \\ \hat{u}_2\left(r,x;2\Psi_{12}b,\frac{1}{2}\Psi_{12}^{-1}a\right), & r \geq r_\mathrm{m}. \end{cases} \tag{63}$$

The relation (62) is satisfied authomatically.

5 CONCLUSION

In this note, we have introduced an alternative approach to calculations of wave excitation in thin disks. Our approach is based on the method of multiple scales and should be understood as an alternative to traditional and rather tedious calculations based on the method of matched asymptotic expansions. The main advantage of this method is in obtaining *global* solutions, what is especially useful in cases when one is interested in global properties of the excited waves rather than in the process of excitation itself. The main applications of this method therefore include properties of trapped or partially trapped oscillations (modes). Another interesting feature of our global solution is that it clearly separates short–scale changes characteristic for waves behavior and the long–scale changes of wave overall properties such as their amplitudes and phases, as each of them occurs on a different variable. Finally, it has also immediately revealed a non–resonant response of the disk.

We have also presented two particular examples of using the method. In section 4.1, we have studied a discrete spectra of p–mode oscillations trapped close to inner edge in relativistic disks and derived an approximative general formula for their frequencies. Although this formula describes well only fundamental modes and first few overtones due to rather crude approximations we have made, extending its applicability by including higher order therms in description of profiles of orbital and epicyclic frequency is rather straightforward.

In section 4.2, we have revisited a textbook example of a disk response to the time and azimuthally dependent tidal field. Also in this case our method may be useful, especially in the cases when the excited waves maybe trapped or it may interact with other perturbations of the disk. Among possible applications are tidally driven eccentric instabilities during superhump events in dwarf novae (Lubow, 1991) or non–linear excitation of trapped g–modes in warped disks (Kato, 2004; Ferreira and Ogilvie, 2008). In the latter case however, it is necessary to extend our calculations to g–mode oscillations. We plan to revisit these problems in near future.

ACKNOWLEDGEMENTS

This work was supported by the GAČR grant no. 17–16287S.

REFERENCES

Abramowicz, M. A., Horak, J. and Kluzniak, W. (2007), Modulation of the Neutron Star Boundary Layer Luminosity by Disk Oscillations, *Acta Astronomica*, **57**, pp. 1–10.

Ferreira, B. T. and Ogilvie, G. I. (2008), On an excitation mechanism for trapped inertial waves in discs around black holes, *Mounthly Notices Roy.Astronom.Soc.*, **386**, pp. 2297–2310, arXiv: 0803.1671.

Goldreich, P. and Tremaine, S. (1979), The excitation of density waves at the Lindblad and corotation resonances by an external potential, *Astrophys.J.*, **233**, pp. 857–871.

Horák, J. (2005), A possible mechanism for QPOs modulation in neutron star sources, *Astronomische Nachrichten*, **326**, pp. 845–848, arXiv: astro-ph/0511569.

Kato, S. (2004), Resonant Excitation of Disk Oscillations by Warps: A Model of kHz QPOs, *PASJ*, **56**, pp. 905–922, arXiv: astro-ph/0409051.

Kato, S. and Fukue, J. (1980), Trapped Radial Oscillations of Gaseous Disks around a Black Hole, *PASJ*, **32**, p. 377.

Lubow, S. H. (1991), A model for tidally driven eccentric instabilities in fluid disks, *Astrophys.J.*, **381**, pp. 259–267.

Nowak, M. A. and Wagoner, R. V. (1991), Diskoseismology: Probing accretion disks. I - Trapped adiabatic oscillations, *Astrophys.J.*, **378**, pp. 656–664.

Paczynski, B. (1987), Possible relation between the X-ray QPO phenomenon and general relativity, *Nature*, **327**, p. 303.

Wagoner, R. V. (1999), Relativistic diskoseismology., *Physics Reports*, **311**, pp. 259–269, arXiv: astro-ph/9805028.

Zhang, H. and Lai, D. (2006), Wave excitation in three-dimensional discs by external potential, *Mounthly Notices Roy.Astronom.Soc.*, **368**, pp. 917–934, arXiv: astro-ph/0510069.